



Received 28 August 2019
Accepted 18 September 2019

Edited by B. Therrien, University of Neuchâtel,
Switzerland

Keywords: crystal structure; Hofmann clathrate;
iron(II).

Supporting information: this article has
supporting information at journals.iucr.org/e

Crystal structure of poly[[diaquatetra- μ_2 -cyanido- iron(II)platinum(II)] acetone disolvate]

Iryna S. Kuzevanova,^{a,b,*} Dina D. Naumova,^b Kateryna V. Terebilenko,^b Sergiu Shova^c and Il'ya A. Gural'skiy^{b,d}

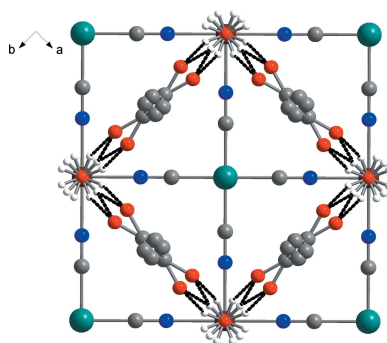
^aDepartment of General and Inorganic Chemistry, National Technical University of Ukraine "Igor Sikorsky Kyiv Polytechnic Institute", Prosp. Peremogy 37, Kyiv 03056, Ukraine, ^bDepartment of Chemistry, Taras Shevchenko National University of Kyiv, Volodymyrska St. 64, Kyiv 01601, Ukraine, ^cDepartment of Inorganic Polymers, "Petru Poni" Institute of Macromolecular Chemistry, Romanian Academy of Science, Aleea Grigore Ghica Voda 41-A, Iasi 700487, Romania, and ^dUkrOrgSyntez Ltd, Chervonotkatska St., 67, Kyiv 02094, Ukraine. *Correspondence e-mail:
iryna.kuzevanova@univ.kiev.ua

In the title polymeric complex, $\{[\text{FePt}(\text{CN})_4(\text{H}_2\text{O})_2]\cdot 2\text{C}_3\text{H}_6\text{O}\}_n$, the Fe^{II} cation has an octahedral $[\text{FeN}_4\text{O}_2]$ geometry being coordinated by two water molecules and four cyanide anions. The Pt cation is located on an inversion centre and has a square-planar coordination environment formed by four cyanide groups. The tetracyanoplatinate anions bridge the Fe^{II} cations to form infinite two-dimensional layers that propagate in the bc plane. Two guest molecules of acetone per Fe^{II} are located between the layers. These guest acetone molecules interact with the coordinated water molecules via $\text{O}-\text{H}\cdots\text{O}$ hydrogen bonds.

1. Chemical context

Hofmann clathrates and their analogues form one of the most famous families of compounds that are able to incorporate guest molecules. The first clathrate was obtained by Hofmann and Küspert in 1897 (Hofmann & Küspert, 1897) and was of composition $[\text{Ni}(\text{NH}_3)_2\text{Ni}(\text{CN})_4]\cdot 2\text{C}_6\text{H}_6$. It was a 2D coordination compound formed by infinite cyanometallic layers that propagate along the ab plane. The 2D system was supported by ammine axial ligands, and guest molecules of benzene were trapped between the layers.

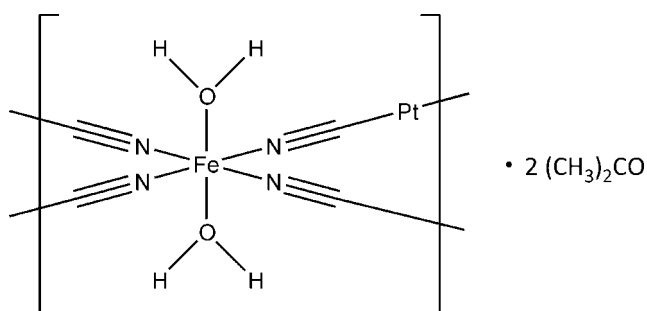
Later, by slight modifications of the chemical composition, several analogous compounds were obtained, leading to the creation of a new class of coordination materials. The first modification was the substitution of nickel with other transition metals, as well as the introduction of other small aromatic guest molecules that resulted in the creation of compounds with the general formula $[\text{M}(\text{NH}_3)_2\text{M}'(\text{CN})_4]\cdot 2\text{G}$ (where $\text{M} = \text{Mn, Fe, Co, Ni, Cu, Zn, Cd, M}' = \text{Ni, Pd, Pt}$ and $\text{G} = \text{benzene, pyrrole, thiophene, aniline, biphenyl, etc.}$; Iwamoto, 1996). The second modification of the Hofmann clathrate was the substitution of square-planar $\{\text{M}'(\text{CN})_4\}^{2-}$ anions with tetrahedral ($\{\text{M}'(\text{CN})_4\}^{2-}$, $\text{M}' = \text{Cd, Hg}$; Arcis-Castillo *et al.*, 2013), linear ($\{\text{M}'(\text{CN})_2\}^-$, $\text{M}' = \text{Cu, Ag, Au}$; Gural'skiy, Golub *et al.*, 2016; Gural'skiy, Shylin *et al.*, 2016), octahedral ($\{\text{M}'(\text{CN})_6\}^{3-}$, $\text{M}' = \text{Co, Cr}$; Dommann *et al.*, 1990) and even dodecahedral ($\{\text{M}'(\text{CN})_8\}^{4-}$, $\text{M}' = \text{W, Nb}$; Ohkoshi *et al.*, 2013) fragments. Additionally, a very important modification was made by the introduction of other organic ligands instead of ammonia. For example, by the introduction of pyridine, the first Fe^{II} -based clathrate $[\text{Fe}(\text{py})_2\{\text{Pt}(\text{CN})_4\}]$ exhibiting spin-crossover (SCO) behaviour was obtained by Kitazawa *et al.* (1996). At the same



OPEN ACCESS

time, the introduction of various bidentate ligands such as pyrazine (Niel *et al.*, 2001; Gural'skiy, Shylin *et al.*, 2016), pyrimidine (Agustí *et al.*, 2008), bis(4-pyridyl)acetylene (Agustí *et al.*, 2008) and others allowed the formation of 3D SCO networks.

Additionally, the characteristics of spin transition in coordination compounds are known to be extremely sensitive to any changes in the chemical environment. As Hofmann clathrate analogues are very easy to modulate, numerous SCO complexes with very different temperatures, abruptnesses and hystereses of SCO were obtained. Moreover, the ability of Hofmann clathrate analogues to incorporate guest molecules provided SCO-based chemical sensors (Ohba *et al.*, 2009).



Herein we present a new Fe–Pt Hofmann clathrate analogue $[\text{Fe}(\text{H}_2\text{O})_2\{\text{Pt}(\text{CN})_4\}] \cdot 2(\text{CH}_3)_2\text{CO}$.

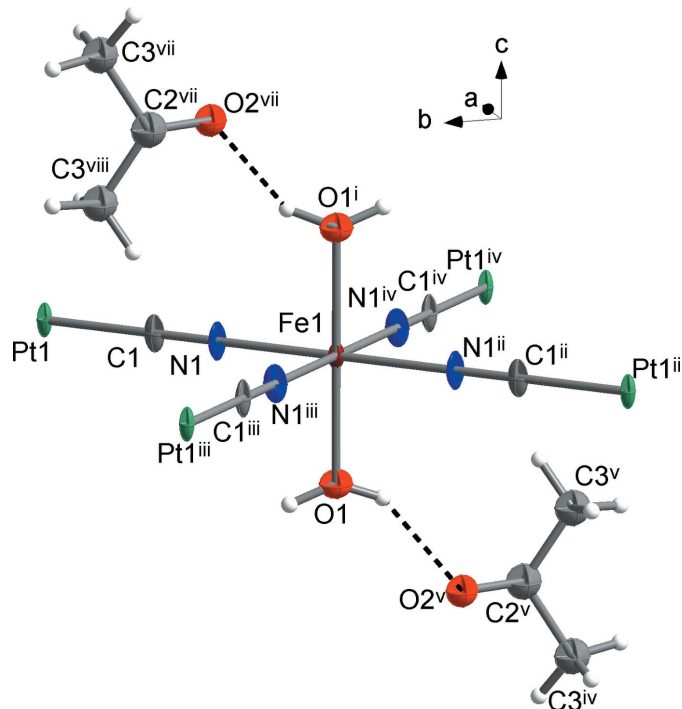


Figure 1

A fragment of the molecular structure of the title compound showing the atom-labelling scheme. Displacement ellipsoids are drawn at the 50% probability level [symmetry codes: (i) $x, -y, 1 - z$; (ii) $-x, -y, z$; (iii) $x, -y, z$; (iv) $-x, y, z$; (v) $-1 + x, -y, z$; (vi) $-1 + x, -y, -z$; (vii) $1 - x, y, 1 + z$; (viii) $1 - x, y, 1 - z$].

2. Structural commentary

The title compound crystallizes in the $P4/mmm$ space group. The Fe^{II} cation has a $[\text{FeN}_4\text{O}_2]$ coordination environment (Fig. 1) comprising four CN^- anions in the equatorial positions [$\text{Fe1}-\text{N1} = 2.158(5)$ Å] and two water molecules in the axial positions [$\text{Fe1}-\text{O1} = 2.130(6)$ Å]. The $\text{Fe}-\text{O}$ bonds are slightly shorter than the $\text{Fe}-\text{N}$ bonds, thus leading to a compressed octahedral geometry. Judging by the bond length, the Fe^{II} cation is in a high-spin state at the experimental temperature (180 K). This is corroborated by the presence of H_2O molecules in the coordination sphere of Fe^{II} . The cyanide anions connect the Fe^{II} and Pt^{II} cations into infinite two-dimensional layers. The Pt^{II} cation is located at a fourfold rotation axis and possesses a square-planar geometry [$\text{Pt1}-\text{C1} = 1.993(6)$ Å, $\text{C1}-\text{Pt1}-\text{C1} = 90^\circ$]. Thanks to the tetragonal symmetry of the crystalline compound, no deviation from an ideal octahedron is observed for Fe^{II} , $\Sigma|90 - \theta| = 0^\circ$, where θ is the $\text{N}-\text{Fe}-\text{N}$ or $\text{O}-\text{Fe}-\text{N}$ angles. Additionally, the compound incorporates two guest molecules of acetone per Fe^{II} centers.

3. Supramolecular features

The crystalline structure is connected by bridging tetracyanoplatinate moieties, which form a two-dimensional grid that propagates along the ab plane (Fig. 2). As imposed by

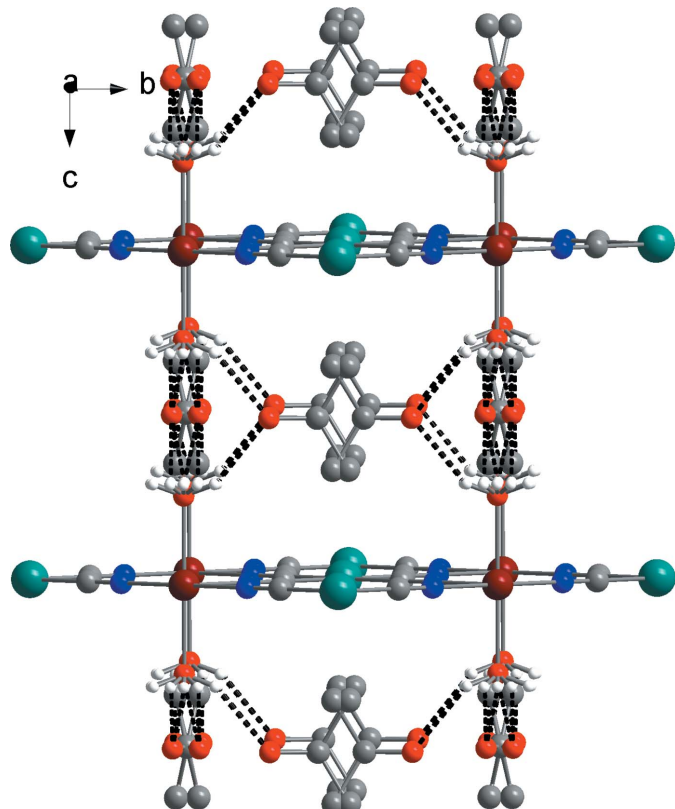


Figure 2

View of the crystal structure of the title compound in the bc plane showing the two-dimensional cyanometallic layers. Hydrogen bonds are shown as dashed lines. Acetone H atoms are omitted for clarity.

Table 1
Hydrogen-bond geometry (\AA , $^\circ$).

$D-\text{H}\cdots A$	$D-\text{H}$	$\text{H}\cdots A$	$D\cdots A$	$D-\text{H}\cdots A$
O1—H1A···O2 ⁱ	0.84	2.03	2.775 (11)	147
O1—H1A···O2 ⁱⁱ	0.84	2.03	2.775 (11)	148
O1—H1B···O2 ⁱⁱⁱ	0.85	2.04	2.775 (11)	144
O1—H1B···O2 ^{iv}	0.85	2.14	2.775 (11)	131

Symmetry codes: (i) $-x+1, -y, z$; (ii) $-x+1, y, -z$; (iii) $-y, -x+1, -z$; (iv) $y, -x+1, z$.

symmetry, no deviation from linearity for the Fe—N—C—Pt linkages is observed [Fe—N—C = 180° , N—C—Pt = 180° , C—Pt—C = 180°]. The distance between parallel cyanometallic layers is 7.973 (6) \AA . The guest acetone molecules are located between the cyanometallic layers. Each oxygen atom of the coordinated water molecules interacts with acetone by O—H···O hydrogen bonds (Fig. 3, Table 1), creating a three-dimensional supramolecular framework. The size of the available voids between the cyanometallic layers allows the acetone molecules to rotate freely, thus leading to disorder of the acetone molecules over four positions.

4. Database survey

A survey of the Cambridge Structural Database (Version 5.38; Groom *et al.*, 2016) confirmed that the title compound has never been published before. It revealed 51 cyanometallic structures of the general formula $[TM(\text{H}_2\text{O})_2\{\text{TM}(\text{CN})_4\}]$, where TM = any transition metal. There were also 19 hits for structures containing $[\text{Fe}[\text{Pt}(\text{CN})_4]]$ fragments: refcodes: OVILEM, OVIRUI, OVIRUI01, OVIRUI02 and OVIRUI03 (Sciortino *et al.*, 2017), AMIJOX (Kucheriv *et al.*, 2016), BEDWEO and BEDWIS (Sciortino *et al.*, 2012), CEMYUQ

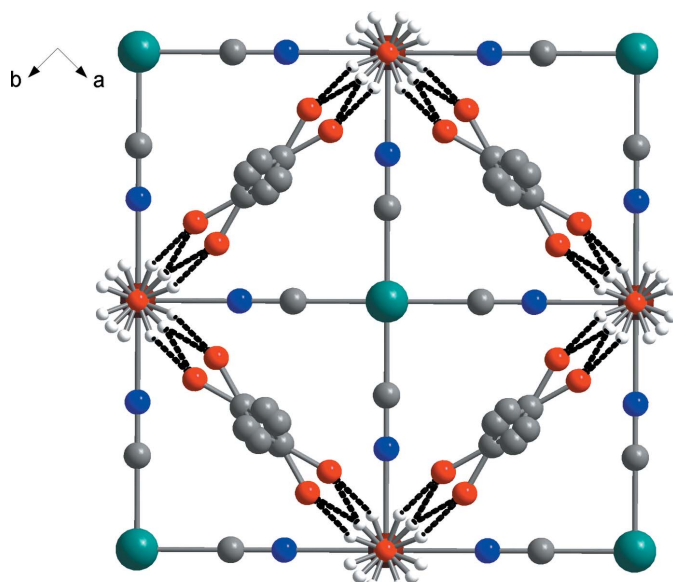


Figure 3

View of the structure of the title compound in the ab plane showing the distortion of the acetone guest molecules. Hydrogen bonds are shown as dashed lines. Acetone H atoms are omitted for clarity.

Table 2
Experimental details.

Crystal data	
Chemical formula	$[\text{FePt}(\text{CN})_4(\text{H}_2\text{O})_2]\cdot 2\text{C}_3\text{H}_6\text{O}$
M_r	507.21
Crystal system, space group	Tetragonal, $P4/mmm$
Temperature (K)	180
a, c (\AA)	7.4802 (4), 7.9725 (11)
V (\AA^3)	446.09 (8)
Z	1
Radiation type	Mo $K\alpha$
μ (mm^{-1})	8.66
Crystal size (mm)	0.05 \times 0.05 \times 0.02
Data collection	
Diffractometer	Rigaku Oxford Diffraction Xcalibur, Eos
Absorption correction	Multi-scan (<i>CrysAlis PRO</i> ; Rigaku OD, 2015)
T_{\min}, T_{\max}	0.699, 1.000
No. of measured, independent and observed [$I > 2\sigma(I)$] reflections	1126, 361, 359
R_{int}	0.037
$(\sin \theta/\lambda)_{\text{max}}$ (\AA^{-1})	0.682
Refinement	
$R[F^2 > 2\sigma(F^2)], wR(F^2), S$	0.025, 0.046, 1.04
No. of reflections	361
No. of parameters	34
H-atom treatment	H-atom parameters constrained
$\Delta\rho_{\text{max}}, \Delta\rho_{\text{min}}$ ($e \text{\AA}^{-3}$)	1.25, -1.06

Computer programs: *CrysAlis PRO* (Rigaku OD, 2015), *SHELXT* (Sheldrick, 2015a), *SHELXL* (Sheldrick, 2015b) and *OLEX2* (Dolomanov *et al.*, 2009).

(Muñoz-Lara *et al.*, 2013), MUHMEI, MUHNAF, MUHNAF01, MUHNAF02, MUHPAH and MUHPAH01 (Martínez *et al.*, 2009), QADDUX (Sakaida *et al.*, 2016), QOJWIW and QOJWIW01 (Cobo *et al.*, 2008) and TURXIP (Ohtani *et al.*, 2013).

5. Synthesis and crystallization

Crystals of the title compound were obtained by slow diffusion (three layers) in a 3 ml tube. The first layer contained 19 mg (0.05 mmol) of $\text{K}_2[\text{Pt}(\text{CN})_4]$ in 0.5 ml of water. The middle layer contained 1.5 ml of a water:acetone (1:1) solution. The third layer contained 25 mg (0.05 mmol) of $\text{Fe}(\text{OTs})_2\cdot 6\text{H}_2\text{O}$ in 0.4 ml of acetone and 0.1 ml of water. The colourless crystals grew in the middle layer within three weeks and were kept in the mother solution prior to measurements.

6. Refinement

Crystal data, data collection and structure refinement details are summarized in Table 2. All hydrogen atoms were fixed at calculated positions and refined as riding with $\text{C}-\text{H} = 0.96 \text{\AA}$ and $\text{O}-\text{H} = 0.84 \text{\AA}$, $U_{\text{iso}}(\text{H}) = 1.5U_{\text{iso}}(\text{C}, \text{O})$. The OH group and the idealized methyl group were refined as rotating.

Funding information

Funding for this research was provided by: Ministry of Education and Science of Ukraine (grant No. 19BF037-01M; grant No. 19BF037-01).

References

- Agustí, G., Thompson, A. L., Gaspar, A. B., Muñoz, M. C., Goeta, A. E., Rodríguez-Velamazán, J. A., Castro, M., Burriel, R. & Real, J. A. (2008). *Dalton Trans.* pp. 642–649.
- Arcís-Castillo, Z., Muñoz, M. C., Molnár, G., Bousseksou, A. & Real, J. A. (2013). *Chem. Eur. J.* **19**, 6851–6861.
- Cobo, S., Ostrovskii, D., Bonhommeau, S., Vendier, L., Molnár, G., Salmon, L., Tanaka, K. & Bousseksou, A. (2008). *J. Am. Chem. Soc.* **130**, 9019–9024.
- Dolomanov, O. V., Bourhis, L. J., Gildea, R. J., Howard, J. A. K. & Puschmann, H. (2009). *J. Appl. Cryst.* **42**, 339–341.
- Dommann, A., Vetsch, H. & Hulliger, F. (1990). *Acta Cryst. C* **46**, 1994–1996.
- Groom, C. R., Bruno, I. J., Lightfoot, M. P. & Ward, S. C. (2016). *Acta Cryst. B* **72**, 171–179.
- Gural'skiy, I. A., Golub, B. O., Shylin, S. I., Ksenofontov, V., Shepherd, H. J., Raithby, P. R., Tremel, W. & Fritsky, I. O. (2016). *Eur. J. Inorg. Chem.* **2016**, 3191–3195.
- Gural'skiy, I. A., Shylin, S. I., Golub, B. O., Ksenofontov, V., Fritsky, I. O. & Tremel, W. (2016). *New J. Chem.* **40**, 9012–9016.
- Hofmann, K. A. & Küspert, F. (1897). *Z. Anorg. Chem.* **15**, 204–207.
- Iwamoto, T. (1996). *J. Incl. Phenom. Macrocycl. Chem.* **24**, 61–132.
- Kitazawa, T., Gomi, Y., Takahashi, M., Takeda, M., Enomoto, M., Miyazaki, A. & Enoki, T. (1996). *J. Mater. Chem.* **6**, 119–121.
- Kucheriv, O. I., Shylin, S. I., Ksenofontov, V., Dechert, S., Haukka, M., Fritsky, I. O. & Gural'skiy, I. A. (2016). *Inorg. Chem.* **55**, 4906–4914.
- Martínez, V., Gaspar, A. B., Muñoz, M. C., Bukin, G. V., Levchenko, G. & Real, J. A. (2009). *Chem. Eur. J.* **15**, 10960–10971.
- Muñoz-Lara, F. J., Gaspar, A. B., Muñoz, M. C., Ksenofontov, V. & Real, J. A. (2013). *Inorg. Chem.* **52**, 3–5.
- Niel, V., Martínez-Agudo, J. M., Muñoz, M. C., Gaspar, A. B. & Real, J. A. (2001). *Inorg. Chem.* **40**, 3838–3839.
- Ohba, M., Yoneda, K., Agustí, G., Muñoz, M. C., Gaspar, A. B., Real, J. A., Yamasaki, M., Ando, H., Nakao, Y., Sakaki, S. & Kitagawa, S. (2009). *Angew. Chem. Int. Ed.* **48**, 4767–4771.
- Ohkoshi, S., Takano, S., Imoto, K., Yoshikiyo, M., Namai, A. & Tokoro, H. (2013). *Nat. Photonics.* **8**, 65–71.
- Ohtani, R., Arai, M., Ohba, H., Hori, A., Takata, M., Kitagawa, S. & Ohba, M. (2013). *Eur. J. Inorg. Chem.* **2013**, 738–744.
- Rigaku OD (2015). *CrysAlis PRO*. Rigaku Oxford Diffraction, Yarnton, England.
- Sakaida, S., Otsubo, K., Sakata, O., Song, C., Fujiwara, A., Takata, M. & Kitagawa, H. (2016). *Nat. Chem.* **8**, 377–383.
- Sciortino, N. F., Scherl-Gruenwald, K. R., Chastanet, G., Halder, G. J., Chapman, K. W., Létard, J.-F. & Kepert, C. J. (2012). *Angew. Chem. Int. Ed.* **51**, 10154–10158.
- Sciortino, N. F., Zenere, K. A., Corrigan, M. E., Halder, G. J., Chastanet, G., Létard, J.-F., Kepert, C. J. & Neville, S. M. (2017). *Chem. Sci.* **8**, 701–707.
- Sheldrick, G. M. (2015a). *Acta Cryst. A* **71**, 3–8.
- Sheldrick, G. M. (2015b). *Acta Cryst. C* **71**, 3–8.

supporting information

Acta Cryst. (2019). E75, 1536-1539 [https://doi.org/10.1107/S2056989019012945]

Crystal structure of poly[[diaquatetra- μ_2 -cyanido-iron(II)platinum(II)] acetone disolvate]

Iryna S. Kuzevanova, Dina D. Naumova, Kateryna V. Terebilenko, Sergiu Shova and Il'ya A. Gural'skiy

Computing details

Data collection: *CrysAlis PRO* (Rigaku OD, 2015); cell refinement: *CrysAlis PRO* (Rigaku OD, 2015); data reduction: *CrysAlis PRO* (Rigaku OD, 2015); program(s) used to solve structure: ShelXT (Sheldrick, 2015a); program(s) used to refine structure: *SHELXL* (Sheldrick, 2015b); molecular graphics: *OLEX2* (Dolomanov *et al.*, 2009); software used to prepare material for publication: *OLEX2* (Dolomanov *et al.*, 2009).

Poly[[diaquatetra- μ_2 -cyanido-iron(II)platinum(II)] acetone disolvate]

Crystal data

[FePt(CN) ₄ (H ₂ O) ₂]·2C ₃ H ₆ O	$D_x = 1.888 \text{ Mg m}^{-3}$
$M_r = 507.21$	Mo $K\alpha$ radiation, $\lambda = 0.71073 \text{ \AA}$
Tetragonal, $P4/mmm$	Cell parameters from 664 reflections
$a = 7.4802 (4) \text{ \AA}$	$\theta = 2.5\text{--}28.5^\circ$
$c = 7.9725 (11) \text{ \AA}$	$\mu = 8.66 \text{ mm}^{-1}$
$V = 446.09 (8) \text{ \AA}^3$	$T = 180 \text{ K}$
$Z = 1$	Plate, clear colourless
$F(000) = 240$	$0.05 \times 0.05 \times 0.02 \text{ mm}$

Data collection

Rigaku Oxford Diffraction Xcalibur, Eos diffractometer	$T_{\min} = 0.699$, $T_{\max} = 1.000$
Radiation source: fine-focus sealed X-ray tube, Enhance (Mo) X-ray Source	1126 measured reflections
Graphite monochromator	361 independent reflections
Detector resolution: 8.0797 pixels mm ⁻¹	359 reflections with $I > 2\sigma(I)$
ω scans	$R_{\text{int}} = 0.037$
Absorption correction: multi-scan (CrysAlisPro; Rigaku OD, 2015)	$\theta_{\max} = 29.0^\circ$, $\theta_{\min} = 2.6^\circ$
	$h = -5 \rightarrow 10$
	$k = -10 \rightarrow 5$
	$l = -10 \rightarrow 5$

Refinement

Refinement on F^2	Primary atom site location: dual
Least-squares matrix: full	Hydrogen site location: mixed
$R[F^2 > 2\sigma(F^2)] = 0.025$	H-atom parameters constrained
$wR(F^2) = 0.046$	$w = 1/[\sigma^2(F_o^2) + (0.0197P)^2]$
$S = 1.03$	where $P = (F_o^2 + 2F_c^2)/3$
361 reflections	$(\Delta/\sigma)_{\max} < 0.001$
34 parameters	$\Delta\rho_{\max} = 1.25 \text{ e \AA}^{-3}$
0 restraints	$\Delta\rho_{\min} = -1.06 \text{ e \AA}^{-3}$

Special details

Geometry. All esds (except the esd in the dihedral angle between two l.s. planes) are estimated using the full covariance matrix. The cell esds are taken into account individually in the estimation of esds in distances, angles and torsion angles; correlations between esds in cell parameters are only used when they are defined by crystal symmetry. An approximate (isotropic) treatment of cell esds is used for estimating esds involving l.s. planes.

Fractional atomic coordinates and isotropic or equivalent isotropic displacement parameters (\AA^2)

	<i>x</i>	<i>y</i>	<i>z</i>	$U_{\text{iso}}^*/U_{\text{eq}}$	Occ. (<1)
Pt1	0.500000	0.500000	0.500000	0.01400 (17)	
Fe1	0.000000	0.000000	0.500000	0.0104 (4)	
O1	0.000000	0.000000	0.2329 (8)	0.0276 (16)	
H1A	0.105309	0.000432	0.196819	0.041*	0.25
H1B	-0.043425	0.098216	0.196839	0.041*	0.125
C1	0.3116 (6)	0.3116 (6)	0.500000	0.0186 (15)	
N1	0.2040 (5)	0.2040 (5)	0.500000	0.0210 (13)	
C3	0.475 (9)	0.036 (8)	0.1546 (18)	0.08 (2)	0.25
H3A	0.473348	0.162844	0.175407	0.114*	0.25
H3B	0.531096	-0.023709	0.246770	0.114*	0.25
H3C	0.354004	-0.005924	0.142949	0.114*	0.25
O2	0.7276 (18)	0.043 (3)	0.000000	0.055 (5)	0.25
C2	0.574 (2)	0.000000	0.000000	0.055 (5)	0.5

Atomic displacement parameters (\AA^2)

	U^{11}	U^{22}	U^{33}	U^{12}	U^{13}	U^{23}
Pt1	0.00585 (17)	0.00585 (17)	0.0303 (3)	0.000	0.000	0.000
Fe1	0.0068 (5)	0.0068 (5)	0.0177 (10)	0.000	0.000	0.000
O1	0.030 (2)	0.030 (2)	0.023 (4)	0.000	0.000	0.000
C1	0.0092 (18)	0.0092 (18)	0.037 (4)	0.003 (2)	0.000	0.000
N1	0.0121 (16)	0.0121 (16)	0.039 (4)	-0.005 (2)	0.000	0.000
C3	0.04 (4)	0.13 (5)	0.056 (9)	-0.03 (2)	0.013 (14)	-0.05 (2)
O2	0.019 (4)	0.109 (15)	0.036 (6)	-0.005 (10)	0.000	0.000
C2	0.019 (4)	0.109 (15)	0.036 (6)	-0.005 (10)	0.000	0.000

Geometric parameters (\AA , $^\circ$)

Pt1—C1 ⁱ	1.993 (6)	Fe1—N1 ^v	2.158 (5)
Pt1—C1	1.993 (6)	Fe1—N1 ^{vi}	2.158 (5)
Pt1—C1 ⁱⁱ	1.993 (6)	Fe1—N1	2.158 (5)
Pt1—C1 ⁱⁱⁱ	1.993 (6)	C1—N1	1.138 (8)
Fe1—O1 ^{iv}	2.130 (6)	C3—C2	1.46 (4)
Fe1—O1	2.130 (6)	O2—O2 ^{vii}	0.64 (5)
Fe1—N1 ^{iv}	2.158 (5)	O2—C2	1.19 (2)
C1 ⁱ —Pt1—C1 ⁱⁱ	90.0	O1 ^{iv} —Fe1—N1 ^{vi}	90.0
C1 ⁱⁱ —Pt1—C1	90.0	N1 ^{iv} —Fe1—N1 ^{vi}	90.0
C1 ⁱ —Pt1—C1	180.0	N1—Fe1—N1 ^{vi}	90.0

C1 ⁱ —Pt1—C1 ⁱⁱⁱ	90.0	N1 ^{iv} —Fe1—N1 ^v	90.0
C1 ⁱⁱⁱ —Pt1—C1	90.0	N1—Fe1—N1 ^{iv}	180.0
C1 ⁱⁱ —Pt1—C1 ⁱⁱⁱ	180.0	N1—Fe1—N1 ^v	90.0
O1—Fe1—O1 ^{iv}	180.0	N1 ^{vi} —Fe1—N1 ^v	180.0
O1—Fe1—N1	90.0	N1—C1—Pt1	180.0
O1—Fe1—N1 ^{vi}	90.0	C1—N1—Fe1	180.0
O1 ^{iv} —Fe1—N1 ^v	90.0	O2 ^{vii} —O2—C2	74.4 (12)
O1 ^{iv} —Fe1—N1	90.0	O2 ^{vii} —C2—C3	123 (2)
O1—Fe1—N1 ^v	90.0	O2—C2—C3	116 (2)
O1—Fe1—N1 ^{iv}	90.0	O2—C2—O2 ^{vii}	31 (2)
O1 ^{iv} —Fe1—N1 ^{iv}	90.0		

Symmetry codes: (i) $-x+1, -y+1, -z+1$; (ii) $y, -x+1, -z+1$; (iii) $-y+1, x, z$; (iv) $-x, -y, -z+1$; (v) $-y, x, z$; (vi) $y, -x, -z+1$; (vii) $x, -y, z$.

Hydrogen-bond geometry (\AA , $^\circ$)

$D\text{—H}\cdots A$	$D\text{—H}$	$H\cdots A$	$D\cdots A$	$D\text{—H}\cdots A$
O1—H1A ^{viii} —O2 ^{viii}	0.84	2.03	2.775 (11)	147
O1—H1A ^{ix} —O2 ^{ix}	0.84	2.03	2.775 (11)	148
O1—H1B ^x —O2 ^x	0.85	2.04	2.775 (11)	144
O1—H1B ^{xi} —O2 ^{xi}	0.85	2.14	2.775 (11)	131

Symmetry codes: (viii) $-x+1, -y, z$; (ix) $-x+1, y, -z$; (x) $-y, -x+1, -z$; (xi) $y, -x+1, z$.